

**PHENOMENA SIMULATION FOR HEAVY DOPING
AND SURFACE RECOMBINATION VELOCITY**

Fred A. Lindholm
Department of Electrical Engineering
University of Florida
Gainesville, FL 32611

CONTENTS
LIST OF SYMBOLS

1. Introduction
2. Basics
 - 2.1 Quantum
 - 2.2 Statistics
3. High Concentrations
 - 3.1 Fermi Level
 - 3.2 Einstein Relation for Majority Carriers
 - 3.3 NP Product if There is No Energy Gap Narrowing
 - 3.4 Slope of Mobility Edge for Minority Carriers
 - 3.5 Energy Gap
 - 3.6 Minority Carrier Diffusivity and Mobility
 - 3.7 Trapping Model
 - 3.8 Other Parameters
4. Moderate Concentrations
 - 4.1 Fermi Level Saturation and Consequences
 - 4.2 Einstein Relation for the Majority Carriers
 - 4.3 Einstein Relation for the Minority Carriers
 - 4.4 Past Treatments
 - 4.5 Unsolved Problems and Consequences for Computer Simulation
5. Basic Equations for Simulation
 - 5.1 Importance of Time Variations
 - 5.2 Conventional
 - 5.2.1 Counting
 - 5.2.2 Remark on Quasi-Fermi Potentials or Levels
 - 5.3 Modified Basic Equations
 - 5.3.1 Modifications for Computer Solution
 - 5.4 Modifications Needed But Not Available
6. Areal Inhomogeneity and Multi-Dimensional Flow
7. Recommendations and Conclusions
8. References
9. Figure Captions
10. Figures

PRECEDING PAGE BLANK NOT FILMED

**LIST OF SYMBOLS
NOT DEFINED IN TEXT**

a	cutoff distance in derivation of energy-gap model
div	divergence operator
D	diffusivity or displacement flux density (context determines)
e	magnitude of electron charge
E	energy of electrons or electric field (context determines)
E'	kinetic energy of free carriers normalized by kT
E _G	energy gap
F	Fermi level
g	generation rate from external source (does not include thermal generation rate)
grad	gradient operator
kT	thermal energy
kT/e	thermal voltage
I	Fermi integral of order one half
j	convection current density, augmented by subscript N or P means electron or hole current density
m	rest mass of electron
m*	effective (or crystal) mass
N _{AA}	ionized acceptor atom concentration
N _C	effective density of states of conduction band
N _{DD}	ionized donor concentrations
n _i	intrinsic carrier concentration
n	electron concentration (also used as subscript)
p	hole concentration (also used as subscript)
T	absolute temperature
QDS(E)	quantum density of states
QFL	quasi-Fermi level
V	applied potential or internal potential (content determines)
v	total time-varying applied or internal potential
v _N	quasi-Fermi potential for free electrons, equals quasi-Fermi level for free electrons when multiplied by -e, prime denotes normalized with respect to thermal voltage, N subscript replaced by P subscript means hole quasi-Fermi potential
W	energy of bound electron in derivation of model for energy-gap narrowing
α	optical absorption coefficient
γ	kinetic energy of free electrons, normalized by kT
ΔE _G	energy-gap narrowing
ε	dielectric permittivity
λ	optical wavelength or screening length (context determines)
χ	electron affinity
ρ	space charge density
τ	recombination lifetime or relaxation time (when symbol is augmented)

1. INTRODUCTION

We survey the theoretical models now available that characterize heavily doped (highly conducting) regions in silicon and analytical and numerical approaches that try to determine the influence of such regions on the conversion efficiency of solar cells. Heavily doped regions are bounded by adjoining regions. As one example, a physical surface bounds the front surface. This physical surface may consist of a mixture of ohmic-contact metal with either an anti-reflection coating or with a thermal or deposited oxide. As another example the adjoining surface may define a transition between heavily doped and more lightly doped silicon. The interplay between the heavily doped and adjoining regions constitutes a key to designs for improved performance. This will receive attention, as will the multi-dimensionality of variables such as current and mobile-carrier density.

Although dilutely doped silicon is well characterized except for some disagreement about optical absorption coefficients, what exists now for heavily doped silicon and its interplay with adjoining regions is an incomplete theory in which not all contributors to transport, recombination, generation, and trapping are defined. Further the parameters relating to these mechanisms and their values as determined by experiment are subject to various interpretations. The presentation will bear in mind these uncertainties and will treat the characterization of heavily doped silicon not as a theory but rather as an imperfectly articulated and incompletely formalized body of experience. This view is intended to help point the way toward the attainment of a more complete theory of heavily doped silicon and thereby toward more informed designs of solar cells. Because computer programs constitute tools both for design and for estimating performance limits, the review will include some remarks pertinent to existing and developing programs.

2. BASICS

Highly doped silicon differs fundamentally from silicon of dilute doping in several main respects.

2.1 Quantum

As the concentration of shallow impurity atoms increases, their ground-state orbitals begin to overlap (Fig. 1), resulting in a distorted quantum density of states which includes an impurity band (Fig. 2). From an experimental viewpoint, one sees the resulting metal-insulator (or Mott) transition occurring for common dopant species at about 10^{18} cm^{-3} (Fig. 3). The theoretical interpretation of Mott and Davies (1967) involves the warped quantum density of states shown in Fig. 4.

At concentrations above about 10^{19} cm^{-3} , the abundance of majority free carriers and the associated screening yields a quantum density of states that more closely approximates the standard dependence, $\text{QDS}(E) \propto \sqrt{\text{kinetic}}$

energy), which applies for dilute concentrations of the impurity atoms. Experimental evidence supporting this conclusion comes from electronic specific heat and other observations (Keyes 1979) and (Shibib and Lindholm 1980).

The random component of the atomic potential introduced by the approximate random positions assumed by the impurity atoms in the host lattice results in band tails, as Lifshitz (1942) first notes. A portion of these band tails comprises bound quantum states where trapping of majority and minority carriers can occur.

Macroscopic lattice strain introduced by a high concentration of impurity atoms, and the accompanying structural imperfections, in principle can also influence the quantum density of states, mainly through changes in the energy gap.

Thus we conclude: (a) the warped quantum density of states at the lower end of the range of high doping concentrations may decidedly affect device performance, particularly near the edge of the p/n junction transition region and particularly if the device design emphasizes avoidance of high impurity concentrations, as in recent cell designs advanced by Green and Blakers, by Wolf, by Spitzer and co-workers, by Rohatgi and by others ¹⁾; (b) the prevalence of a near standard quantum density of states for concentrations $> 10^{19} \text{ cm}^{-3}$ admits treatment of the majority carriers as a Fermi gas, and associated simple screening models enter; (c) the existence of bound states near the minority-carrier band edge may introduce trapping as an important mechanism if many such states exist.

These conclusions receive attention in the sections that follow.

2.2 Statistics

Electrons (and holes) are fermions. Thus their distribution in energy is described by Fermi statistics. At low enough carrier concentrations, the Fermi function tends toward a Maxwell-Boltzmann function (Boltzmann statistics). Fermi statistics contain Boltzmann statistics. Thus there is no fundamental reason to argue the issue whether Boltzmann or Fermi statistics apply, as many workers have done. The answer is that Fermi statistics always apply. From a practical viewpoint, however, some need exists for further consideration. As one example, if past work has used Boltzmann statistics, correctly or incorrectly, as a vehicle for framing such experimental results as energy-gap narrowing ΔE_G , then one must take care in the introduction of Fermi statistics when using these results. If raw data exist, however, then one can use Fermi statistics to reframe the parameters of interest. Such a parameter is energy-gap narrowing and its dependence on impurity concentration. As

1) See the special issue of the IEEE Transactions Electron Devices, May 1984.

another example, one may wish to avoid Fermi statistics to obtain expressions that yield more easily to analytical or numerical treatment. For numerical solution of the finite-difference or finite-element counterparts of the basic differential equations, however, the availability of a variety of accurate approximations to the related Fermi integrals (Blakemore 1982) apparently makes this unnecessary.

As a fundamental point, one may remember that Fermi statistics always describe electrons or holes. This is not true for Boltzmann statistics which introduce considerable error if the majority-carrier density $> 10^{18} \text{ cm}^{-3}$. Incorrect temperature dependence of variables may be one result of misuse of Boltzmann statistics. We would not belabor this issue if it had been discussed less in the literature.

Fermi statistics also describe the occupancy in equilibrium of bound states, such as those in band tails. But a difficulty enters here because the Fermi statistics must be altered to contain the degeneracy of the bound state. This degeneracy apparently is unknown for band tails. The same difficulty prevails, of course, if one uses Boltzmann statistics.

Finally we define explicitly the term, Fermi gas, used in Sec. 2.1. The concentration of such a gas is determined by the integral of the product of the standard Fermi function for delocalized states and the standard quantum density of state, $QDS \propto \sqrt{\text{kinetic energy}}$. This integral, the Fermi integral to order one-half, will enter later into models for ΔE_G through the screening length of a Fermi gas.

3. HIGH CONCENTRATIONS

By high concentrations of shallow acceptor or donor states we mean $> 10^{19}/\text{cm}^3$, approximately. For such concentrations, as suggested above, the quantum density of delocalized states of both conduction and valence bands obey,

$$QDS(E') \propto \sqrt{E'} dE' \quad (3.1)$$

where E' is the kinetic energy measured from the mobility edge of the band. For developments that follow, note that an electron, or hole, at this band edge has only potential energy, according to quantum theory. Thus the band edge corresponds to the energy reference for kinetic energy.

Thus the hole or electron concentration in thermal equilibrium is the integral, from the band edge to infinity, of the product of (3.1) and the standard Fermi-Dirac function. For the majority carriers this integral, the Fermi integral of order one-half, describes a Fermi gas. Because the Fermi function goes into a Boltzmann distribution for low particle concentrations, the Fermi gas becomes a Boltzmann gas for the minority carriers.

3.1 Fermi Level

The Fermi level F or Fermi potential of a Fermi gas follows from standard expansions (Kubo, 1966, p. 231); the Fermi level shows only a slight temperature dependence, which for terms up to the order T^4 is

$$F(T)/F(T = 0K) = 1 - (\pi^2/12)[kT/F(0)]^2 - (\pi^4/80)[kT/F(0)]^4 + \dots \quad (3.1.1).$$

The weakness of this temperature dependence will prove useful in the discussion below concerning the energy gap, measured electrically.

3.2 Einstein Relation for Majority Carriers

For a position-dependent doping concentration, the principles of detailed balance requires oppositely directed majority-carrier drift and diffusion currents, equal in magnitude, for thermal equilibrium. This requirement, together with the position independence of F and with the association of a band edge with potential energy (discussed in regard to Eq. 3.1), establishes the slope of the majority-carrier band edge and hence the drift field acting on the majority carriers. The energy-gap narrowing $\Delta E_G(x)$ then determines the drift field (or quasi-field) acting on the minority carriers (Fig. 5). In general, the majority-carrier and minority-carrier fields differ in magnitude and may be opposite in sign. This has central importance in the analysis of the performance of devices.

Because of the balance, and for other reasons, the ratio of diffusivity D to mobility μ is significant. For the Boltzmann gas of the minority carriers,

$$D/\mu = kT/e \quad (3.2.1)$$

which is the standard Einstein relation of 1905. If trapping influences the transport of minority carriers, as later we shall suggest, the Einstein relation remains valid because trapping is spontaneous and random.

For majority carriers, the Einstein relation of the Fermi gas shows that D has a stronger dependence on particle density than does μ . Lindholm (1984) has suggested that this behavior originates in the kinetic pressure dependence of a Fermi gas, the gradient of which is related to the gradient of the chemical potential and hence to diffusion. For $T = 300K$, the dependence is shown in Fig. 6, first plotted by Lindholm and Ayers (1968). Landsberg (1952) first derived the D/μ relation for a Fermi gas as a ratio of Fermi integrals, a simple yet accurate approximation of which is due to Kroemer (1978).

3.3 NP Product if there is no Energy Gap Narrowing

The hole concentration product with the electron concentration for thermal equilibrium enters semiconductor device physics because excitations may often be assumed to provoke a small perturbation (quasi-equilibrium) of the equilibrium condition. Thus use of the PN product in equilibrium often yields a pre-exponential constant multiplying a term of the form, $\exp[V/(kT/e)] - 1$.

For a Boltzmann gas,

$$PN = n_i^2(T), \text{ (equilibrium)} \quad (3.3.1)$$

which is often called the law of mass action. For a Fermi gas, the PN product falls with increasing majority carrier density. Kleppinger (1970) first plotted this dependence (Fig. 7). Because

$$n_i^2 = \exp[-(E_G/kT)] \quad , \quad (3.3.2)$$

one might think that Fig. 7 implied an increase in energy gap as the majority carrier concentration increases. But the construction of Fig. 7 assumed independence of the energy gap on majority carrier concentration. Thus the result shown derives only from use of Fermi rather than the more familiar Boltzmann statistics.

Many previous workers have interpreted experimental results using Boltzmann statistics to deduce the carrier concentration dependence of the energy gap. Because of the dependence shown in Fig. 7, when a Fermi gas is used to describe majority carriers, larger energy-gap narrowing is inferred from experimental data. This partly explains the discrepancy between the results of Neugroschel, Pao, and Lindholm (1982) and those of many other workers. A related elaboration appears below.

3.4 Slope of Mobility Edge for Minority Carriers

We have discussed this issue above in Sec. 3.2, relating to the inequality between the drift fields acting on the majority and the minority carriers. For a diffused junction, for example, a huge drift field acts on the majority carriers. If this same field were to act on the minority carriers, those injected over the p/n junction barrier into the quasineutral emitter, or front layer, would be so significantly drifted back toward the junction transition region that the probability of reaching the surface would be low (Lindholm, Li and Sah, 1975). Experimental evidence indicates that such minority carriers reach the surface in great abundance where they vanish, if the front surface recombination velocity is high, without contributing to current in the external circuit (Iles and Sockloff, 1975), (Fossum, Lindholm and Shibib, 1979). The inequality of the majority-carrier and minority-carrier quasi fields helps explain this result.

3.5 Energy Gap

If we restrict consideration to donor or acceptor impurity atom concentrations high enough (Sec. 2.1) that a Fermi gas description becomes adequate, then an approximate model for the energy-gap narrowing ΔE_G as a function of majority-carrier concentration (n or p) emerges. The central parameter entering this model is the Debye or Thomas-Fermi screening length λ , as first suggested by Sah and collaborators (1981) and discussed systematically by Landsberg, Neugroschel, Lindholm and Sah (1984).

The model starts from the view that the highly doped semiconductor is, to some extent, a neutral dielectric continuum in which positive and negative particles are smeared out over macroscopic volume. This model continuum consists implicitly of particles in complicated and correlated motions, the correlation coming from the forces among the particles. The correlated motions of the actual many body problems incorporate the long-range part of the Coulomb forces between the electrons (assuming for concreteness n^+ silicon) and between them and other charges, both those fixed in the lattice (ions) and those that are mobile. The most significant forces are short-range which one can view as forces altered by screening of the many electrons. These forces one can characterize, with no additional approximation involved, as a screened potential, the relation being the equality between the gradient of the scalar potential and the vector force field. The introduction of the screened potential simplifies discussion, as will be seen.

We treat the screening length for this potential as a constant, which is an approximation (Landsberg, et. al., 1984). Then we consider the creation of an electron-hole pair, which at the first instant are in a bound state at $r = 0$, to fix the reference position. Then we imagine the hole to remain trapped and the electron to be removed to infinity against the screened Coulomb attraction. The total energy to create the pair, and to separate it, is (Fig. 9)

$$\text{ENERGY} \equiv W + (e^2/\epsilon a)\exp(-\lambda a) \quad (3.5.1)$$

where W is the energy required to create the pair in the bound state and the second term on the right side is the energy required to separate the pair. The sum of these two energies then yields a created **free** electron and **free** hole. Thus this sum is the energy gap, which depends on n and p through the screening length λ . The consequent energy gap narrowing, $\text{ENERGY}(0,0) - \text{ENERGY}(n,p)$, illustrated in Fig. 9, depends only on $\lambda(n,p)$ because subtraction cancels W and the cut-off distance a (Landsberg et. al., 1984), which are regarded as concentration independent. The energy W is concentration independent because the model employed attributes energy-gap narrowing only to carrier screening.

The question remains as to the choice of λ , a parameter that enters many part of physics (Landsberg, 1981). Using Debye or Thomas-Fermi screening gives the same result in the limit of extreme degeneracy. The result, which in cgs units is

$$\Delta E_G = e^2 \lambda / \epsilon \quad , \quad (3.5.2)$$

is a function of the effective mass of the majority carriers, ϵ , and n for n^+ silicon. If one assumes equality between the effective mass and the rest mass, $\epsilon = 11.7$, one obtains

$$\Delta E_G = 215 (10^{20}/n)^6 \text{ meV} \quad . \quad (3.5.3)$$

This energy-gap narrowing exceeds that of Lanyon and Tuft (1979) who adopted a different screening model and used a different physical picture following the suggestion of Hauser (1969). The difference is a factor of 1.33.

We note the prediction of an energy-gap narrowing of 215 eV for a carrier concentration of $10^{20}/\text{cm}^3$.

For a general value of n , and for a parabolic band (Sec. 2.1), the energy gap becomes

$$\Delta E_G = (e^2/\epsilon) \{ [4\pi e^2/\epsilon kT] N_C I(\gamma) \}^{1/2} \quad (3.5.4)$$

where I is the Fermi integral of order one-half and γ is the kinetic energy of the electrons normalized by kT . If both holes and electrons are numerous, one need only add a similar Fermi integral for the holes multiplied by the effective density of states for the valence band.

This last formula we shall adopt for comparison with experiment. Though it applies for all levels of concentrations, we shall recall our previous discussions (particularly that of Sec. 2.2) emphasizing the inappropriateness of the assumed parabolic bands that underlie the origin of the Fermi integrals of order one half. Moreover, because of physics related to the cutoff distance a in (5.3.1), the expression holds with good accuracy only for concentrations up to $5 \times 10^{20}/\text{cm}^3$ (Landsberg, et al., 1984).

If we now compare with experiment (Fig. 10) obtained by electrical measurements, we note the excellent fit of this theory with the values obtained for Si:As by Neugroschel, Pao, and Lindholm (1982), (full circles), and for Si:B by Landsberg, Neugroschel, Pao, Lindholm and Sah (1984) (full triangles) by the same method. We note that the agreement is good only for majority carrier concentration $> 5 \times 10^{19}/\text{cm}^3$, as expected from the discussions of Sec. 2.1 and elsewhere above. In constructing Fig. 10, we have assumed for the experimental results in full circles and triangles an effective mass of electrons and holes that is a factor of 1.1 larger than the electron rest mass. The effective masses have uncertain values for highly doped silicon, though the assumption just stated agrees with the values usually advanced for the effective electron mass of dilutely doped silicon. In regard to most of the rest of the measurements of energy-gap narrowing in the literature, some of which are shown in Fig. 10 without explicit identification, Boltzmann statistics were used. We have recalculated these data so as to allow a fair comparison.

The agreement between the model above and the various experiments approaches the agreement between different experiments. The agreement tends to be better for larger concentrations, as expected (Sec. 2.1).

The experimental results of workers other than those mentioned are smaller than ours cited above. Apparently several reasons exist for this disagreement. In some of the work of others, the impurity concentration was or

may have been markedly dependent on position. Thus enters the effect of the quasi-field on the minority carriers (Sec. 3.4); moreover these workers used some spatial average of the impurity concentration. Another significant difference between the work referenced above and that of others involves assumptions about the minority carrier mobility μ . The energy-gap narrowing from electrical measurements pictured in Fig. 10 comes from the minority-carrier current, which depends on the product $\mu \exp(\Delta E_G/kT)$. Other workers have assumed an equality between the minority carrier and majority carrier mobility, which has the convenience that the majority carrier mobility is perhaps adequately known from conventional measurements. In contrast, in the work cited above, we assumed only a near temperature independence of μ and ΔE_G in a small range of temperatures near 300 K. This leads to evidence that μ is about one order of magnitude smaller than the majority carrier mobility for concentrations of about $10^{20}/\text{cm}^3$ in Si:As (Neugroschel and Lindholm, 1983). This contributes to the differences noted. Controversy about these issues exists, as evidenced by the communications exchanged between del Alamo and Swanson (1984) and Neugroschel and Lindholm (1984).

Figure 11 compares our model predictions (Eq. 5.3.4) with the recent 5 K photoluminescence and photoluminescence excitation data of Wagner (1984). At 5 K and for these doping concentrations, the effective masses for holes and electrons are unknown. Thus we introduce the noncommittal symbol m^*/m for the effective mass ratio with the electron rest mass. For intrinsic silicon at 5 K, the ratio is about 1.06 (electrons) and 0.59 (holes). Using the temperature dependence implicit in our model above, we find that best agreement with Wagner's data occurs for $m^*/m = 0.45$ (Fig. 11).

3.6 Minority-Carrier Diffusivity and Mobility

Exploiting temperature dependencies, Neugroschel and Lindholm (1983) have presented evidence, as noted above, for a much lower minority-carrier mobility and diffusivity than that assumed previously. They obtained these results for Si:As having a doping concentration of about $10^{20}/\text{cm}^3$, for which a customary Fermi integral of order one-half was assumed to describe the majority electrons. This fixes the electron quasi-Fermi level approximately 100 meV in the conduction band above the band edge. In a simple physical picture advanced to explain these results, Neugroschel and Lindholm supposed the trapping of minority carriers at the bound states of band tails (or at acceptor states in the compensated n^+ silicon). Holes while trapped do not contribute to current of the hole Boltzmann gas. Thus for this mechanism to enter significantly, the characteristic time for thermal emission of a hole from a shallow bound state must be of the same order as the scattering time of holes within the valence band. Although band tails appear near both conduction and valence-band edges, trapping of the majority electrons is a negligible mechanism because the electrons contributing to current lie near the Fermi level, about 100 meV away from the nearest band tail state. An illustration of the pertinent hole trapping appears in Fig. 12.

3.7 Trapping Model

To explore this mechanism from a theoretical viewpoint, it is useful to generalize the Boltzmann equation to include band-bound transitions. This generalization, discussed, for example, by Smith, Janak, and Adler (1967) and worked out in detail by Sah and Lindholm (1973), involves approximating the collision integral, for small departures from equilibrium, by the sum of two terms of the form, $(f - f_0)/\tau(\text{relaxation})$. This first term is the customary relaxation time approximation for the nonequilibrium distribution function f in which $\tau(\text{scattering}) = \tau(\text{relaxation})$ is the scattering time that characterizes intraband transitions. In the second term, $\tau(\text{trapping})$ instead appears, which characterizes the mean trapping time of holes for localized states near the valence-band edge. Thus $\tau(\text{trapping})$ enters into the description of the hole current and of $\mu(\text{holes})$, as described by Sah and Lindholm (1973). In principle, this enables detailed investigations of the trapping model and of the bound states of the minority-carrier band tails.

3.7 Other Parameters

Besides the functional dependencies of the energy-gap narrowing and the minority-carrier mobilities and diffusivities, emphasized in the preceding discussions, other parameters important for solar-cell analysis and design remain uncertain for silicon having donor or acceptor atom concentrations in the moderately high and high ranges. We point to the absorption coefficient $\alpha(\lambda)$, which has importance not only for the obvious reason of detailed calculation of photogeneration in the emitter or front layer. It also has importance in schemes for measuring other parameters. We have not touched on the lifetime in the volume of the heavily doped emitter and have referred only tangentially to the front surface recombination velocity. This is intentional, based on the assumption that other authors in the JPL Research Forum will focus on parameters relating to these mechanisms. In an extensive recent review of electrical current and carrier density in degenerate semiconductors, Marshak and van Vliet (1984) have emphasized the need for better knowledge of such parameters as the effective masses, dielectric permittivity ϵ , and electron affinity χ . We agree with their assessment, and refer the reader to their paper for details.

4. MODERATE CONCENTRATIONS

For impurity concentrations approximately $\sim 10^{18}/\text{cm}^3$, the metal-insulator transition implies that the majority-carrier quantum density of states will differ sharply from the standard dependence. This occurs partly because of the existence of impurity bands, according to the theory that interprets this transition.

Thus many aspects of the physical electronics become more difficult and less precise.

4.1 Fermi Level Saturation and Consequences

The severe warping of the quantum density of states from the rigid-band model (parabolic band) results in far less penetration of the Fermi level into the majority carrier band as the doping concentration increases. Indeed for a range of doping concentrations one may anticipate that the Fermi level nearly saturates. This leads to (a) a smaller energy-gap narrowing than interpretation of data on emitter recombination current by the rigid-band model would imply, and (b) a stronger quasi-field on the holes (minority carriers) that drifts holes toward the surface. This in turn yields a stronger dependence of emitter recombination current (and open-circuit voltage if emitter recombination current is important in a cell design on the front surface recombination velocity).

Figure 13 illustrates result (b) for a concentration of free electrons decreases in the n^+ silicon with x from its value at the surface ($x=0$).

4.2 Einstein Relation for the Majority Carriers

In its simplest derivation, the Einstein relation for D/μ derives from detailed balance between drift and diffusion tendencies in thermal equilibrium. Diffusion depends on the gradient of chemical potential, which is related to the kinetic pressure. The kinetic pressure of a Fermi gas having a non-standard band differs considerably from that for a standard band. Thus so also does the Einstein relation differ from that pictured in Sec. 3.2.

4.3 Einstein Relation for the Minority Carriers

The minority carriers are a Boltzmann gas, and the Einstein ratio is standard: $D/\mu = kT/e$.

4.4 Unsolved Problems and Consequences for Computer Simulation

These issues are treated in Sec. 5.3.

5. BASIC EQUATIONS FOR SIMULATION

The basic equations for analysis or for computer simulation follow from the foregoing discussion of the physics for high concentrations of impurities (Fermi gas for majority carriers). As the discussion has indicated, these equations involve approximations, especially for such parameters as energy-gap narrowing and the minority-carrier diffusivity and mobility. The approximation becomes more severe for the moderate range of dopings, between approximately 10^{18} to 10^{19} per cm^3 , where impurity banding warps the quantum density of states for majority carriers from its standard dependence on energy. Thus the position of the Fermi level and consequently the quasi field for the majority carriers and the temperature dependence of these variables become more

uncertain than they are for the higher range of doping concentration. The Einstein ratio for the majority carriers, the energy-gap narrowing, and other quantum and transport parameters also becomes less accurately known.

5.1 Importance of Time Variations

Although when delivering power a solar cell operates in the steady-state, time variations of the carrier concentrations, quasi-Fermi levels, potential, and particle current still have significance for several reasons. First, for example, many methods of measuring parameters such as lifetime τ involve either a transient or an $\exp(i\omega t)$ variation. As a second example, trapping of minority carriers at bound states in the band tails or at impurity states in compensated silicon may play a role in determining the minority-carrier diffusivity D and mobility μ . As a third example, inclusion of the full set of the Maxwell equations among the basic equations, when combined with phenomenological parameters such as ϵ , in principle yields reflection and transmission at the heavily doped surface.

5.2 Conventional Equations

In the absence of the effects indicated in the preceding sections that make the physical electronics of heavily doped silicon differ from the physical electronics of dilute silicon, the conventional equations are:

$$\partial n / \partial t = \text{div}(j_N / -e) - R_n + g(\text{external}) \quad (5.2.1)$$

$$\partial p / \partial t = \text{div}(j_p / e) - R_p + g(\text{external}) \quad (5.2.2)$$

$$j_N = e\mu_n E + eD_n \text{grad}(n) \quad (5.2.3)$$

$$= -e\mu_n n \text{grad}(v_N) \quad (5.2.3a)$$

$$j_p = e\mu_p E - eD_p \text{grad}(p) \quad (5.2.4)$$

$$= -e\mu_p p \text{grad}(v_p) \quad (5.2.4a)$$

$$\text{div}(D) = \rho \quad (5.2.5)$$

$$= e(p - n + N_{DD} - N_{AA}) \quad (5.2.5a)$$

$$j = j_N + j_p + \partial D / \partial t \quad (5.2.6)$$

If recombination dominates, the removal rates, R_n and R_p become equal. For electrons and holes from quasineutral regions, this equality defines the lifetime τ : ($R \rightarrow \Delta n / \tau$).

A seventh equation will describe, for the steady state, some assumed model for the recombination rate and hence the lifetime τ . Sah (1977) has expressed this equation in its most general form to unify impact-Auger, Shockley-Read-

Hall and other mechanisms. For greater generality, the kinetic rate equation for the time variation of particle density on traps (Sah 1971) supplements the equation of the steady state recombination rate. This then provides a quantitative characterization of the minority carrier diffusivity D and mobility μ when the trapping rate at bound states becomes comparable to the scattering rate within the minority carrier band (Sah and Lindholm, 1973), as discussed earlier. This equation, or equations, not given explicitly here, is numbered (5.2.7).

To these seven equations are added auxiliary relations to enable or aid solution.

$$\text{div}(j + \partial D/\partial t) = 0 \quad (5.2.8)$$

$$E = -\text{grad}(V) \quad (5.2.9)$$

$$E = D/\epsilon \quad (5.2.10)$$

$$n/n_i = \exp(v' - v'_N) \quad (5.2.11)$$

$$p/n_i = \exp(v'_p - v') \quad (5.2.12)$$

$$\text{diffusivity/mobility} = kT/e \quad (5.2.13)$$

Here the primes denote normalization by the thermal voltage kT/e to yield a dimensionless variable. Eq. (5.2.8) assures the position independence of the total current, which becomes the position independence of convection current j for the steady state and $j \neq f(x)$ in a one-dimensional model. This relation simplifies analysis. Maxwell's other three equations are added, but not shown, for reasons given directly above.

We omit detailed discussion of the lifetime τ for heavily doped silicon, assuming that other authors in this Research Forum will provide this.

5.2.1 Counting

To assess the possibility of solution, we now count unknowns and equations. The first two equations, (5.2.1) and (5.2.2), the continuity equations for holes and electrons, introduce four unknowns: the electron and hole densities and current densities. The optical excitation determines the generation rate through a relation of the form,

$$g(\text{external}) \propto \int \exp[-\alpha(\lambda)x] d\lambda \quad (5.2.14)$$

where the constant of proportionality depends on the fraction of the sunlight transmitted past the surface into the volume of the solar cell. For a given solar-cell design, $g(\text{external})$ is assumed known.

If we deal with the current densities as expressed in terms of drift and diffusion components, we introduce one more unknown: the electric field $E(x) = -\text{grad}[v(x)]$. Assuming ϵ is known in (5.2.10), (5.2.5a) then becomes Poisson's equation for $v(x)$, the fifth equation in five unknowns.

If we deal with the electron and hole currents expressed in terms of the gradient of their quasi-Fermi potentials, we have as unknowns, in the two current density and two continuity equations, the following: the hole and electron densities, and the hole and electron quasi-Fermi potentials, and the hole and electron current densities. This gives six unknowns in four equations. But (5.2.11) and (5.2.12) introduce only a single additional unknown, $v(x)$, the electric potential. Thus adding Poisson's equation, from combining (5.2.5a), (5.2.9) and (5.2.10), yields in principle a solvable set of equations.

The equations are nonlinear. To illustrate this, note that the product of n and $\text{grad}(-v(x))$ appears in the equation for the electron current density. But n and v are related through (5.2.5) when put in the form of Poisson's equation. Assuming analytic functions, one can express this relation by a Taylor series. Thus the equation for electron density involves a sum in which $n, n^2, n^3, n^4, n^5 \dots$ appear.

Because of nonlinearity, solution of the basic equations requires either approximations for special cases that yield analytic solutions or numerical solutions of the finite-difference or finite-element counterparts of the basic equations.

5.2.2 Remark on Quasi-Fermi Potentials or Levels

Solar cells must contain ohmic contacts to enable power delivery. An ohmic contact is a union between metal and semiconductor that allows electrons and holes to flow freely between the metal and the semiconductor. Hence, at the contact, electrons and holes can neither accumulate or become depleted, their densities stay at equilibrium values (assumed known), and the hole and electron quasi-Fermi levels converge to the Fermi level F . This implies that at an ohmic contact the merged quasi-Fermi levels in the semiconductor join the Fermi level in the metal without discontinuity. But the Fermi level at any point in a metal is the electric potential at that point. Thus the potential difference between two ohmic contacts in a solar cell or any semiconductor device equals the difference between the merged quasi-Fermi levels in the semiconductor at the two contacts.

As a result, a potential difference in an external circuit causes an equal potential difference in the quasi-Fermi levels at the two contacts. Hence use of the quasi-Fermi level description of hole and electron currents allows a simple introduction of the boundary conditions on electric potential. The alternate description in terms of drift and diffusion components requires satisfaction of the boundary conditions on potential by setting a line integral of the electric field through the semiconductor equal to the potential difference appearing at the terminals.

Advantages thus apparently result for numerical simulation. Moreover a preference for description in terms of quasi-Fermi levels enables a straightforward introduction of trapped particles at bound states in the forbidden gap. This is done by use of quasi-Fermi levels (or occupancy probabilities) for each of the bound states. If then one restricts attention first to variations in the potentials at the terminals and hence to variations in the quasi-Fermi potentials within the volume of the semiconductor device that are much smaller than the thermal voltage kT/e , the set of basic equations become linear. To these linear equations corresponds a electric circuit representation. That circuit representation often can be simplified by using the theory of electric circuits; for example, Y to Δ transformations can yield simplifications. Thus numerical solution of the finite difference equations becomes easier. To obtain solutions to the nonlinear equations, one simply adds the consequences of successive small-signal responses to potentials small relative to kT/e .

Sah has advanced and utilized computer algorithms related to those just described; for example, see Sah (1971) and Sah, et al. (1981).

5.3 Modified Basic Equations

We now consider the modifications needed to include the phenomena occurring in highly doped silicon treated in the foregoing sections. The reader may refer to Sec. 5.2 on the conventional basic equations, which we now modify.

The continuity equations remain intact; they serve the bookkeeping purpose of summing all contributors to changes in particle density with time.

Because carriers at the mobility edge have only potential energy, we see that the electric field E governing the drift component of the majority-carrier current becomes $\text{grad}[\text{mobility edge}/-e]$. This is the same relation prevailing in the conventional equations except that the mobility edge has replaced the band edge. If we take n^+ material for concreteness of discussion

$$E \rightarrow -\text{grad}[E_C / -e] \quad , \quad (5.3.1)$$

where

$$\text{grad}[E_C / -e] = \text{grad}(v) + \text{grad}(\chi / -e) \quad (5.3.2)$$

as in Sah and Lindholm (1977) and Marshak and van Vliet (1984).

Typically majority carrier concentrations will be perturbed only slightly in nonequilibrium; that is, the low-injection condition will prevail. Thus we anticipate a near position independence of the majority-carrier quasi-Fermi level, and we anticipate that the energy separating this quasi-Fermi level from the mobility edge for the majority-carrier band will remain as in equilibrium, to a good approximation. Thus the left side of (5.3.2) will be determined; the right side will become unimportant to the majority-carrier drift component.

For a Fermi gas (parabolic band), the diffusion component of the majority carriers remains intact; the D/μ ratio reflects the Fermi statistics, as discussed in Sec. 3.2. For a moderately doped region, we have emphasized the warping of the quantum density of states, in accord with the metal-insulator transition. The diffusion current then depends on the random force (Prigogine, 1980) or kinetic pressure appropriate to this quantum density of states. To account for this the diffusion component of the majority carrier current, a term involving a gradient in addition to the gradient of n appears (Marshak and van Vliet, 1984).

We note that these complications concerning the majority-carrier diffusion current vanish if one deals with (5.2.3a) in which this current is simply the electron conductivity times the gradient of the electron quasi-Fermi potential (electrochemical potential). The electrochemical potential is a basic thermodynamic variable whose gradient is linear in the particle current except for large deviations from equilibrium. The vanishing of the complications referred to is only apparent, however, because they will reappear in the relation between the quasi-Fermi levels and the particle densities, as we shall soon see.

Equation (5.3.1), for the majority carriers, relates to the drift component of hole current (minority current) through

$$\text{grad}[E_V/-e] = \text{grad}[E_G/-e] - \text{grad}[E_C/-e] \quad . \quad (5.3.3)$$

The product of this gradient (left side) times the hole conductivity determines the hole drift current (minority-carrier drift current) in terms of the gradient of the majority-carrier mobility edge (known through Eq. (5.3.1)) and the energy gap dependence, assumed known through the model of Sec. 3.5 or through experimental determination.

If we assume that the band tails of the minority-carrier band are mainly bound states, the hole (minority-carrier) current is the conventional sum of drift and diffusion components, with $D/\mu = kT/e$, for a Boltzmann gas.

Thus the conventional description for the minority-carrier current survives except that the gradient of the quasi-field, influenced by the gradient of the energy gap, replaces the conventional electric field. This replacement has key importance, as we have emphasized earlier. But the survival of a simple description of the minority-carrier current permits, for the quasi-neutral emitter, many approximations that give simple relations for the quasineutral emitter recombination current. Examples include the transparent-emitter model of Shibib, Lindholm, and Therez (1979) extended by del Alamo and Swanson (1984), the field-free model introduced by Fossum, Lindholm, and Shibib (1979), etc.

5.3.1 Modifications for Computer Solution

Having just discussed analytic solutions for the quasineutral regions, we now turn attention again to contact-to-contact computer solution by finite-difference or equivalent formulations of the basic equations.

Consider Poisson's equation, resulting from combining (5.2.5a) with (5.2.9) and (5.2.10). The key issue becomes the relation of potential $v(x)$ to $n(x)$ and $p(x)$ in view of (5.3.2). Consideration that p and n are proportional to integrals of the form, $\int [QDS(E)](\text{probability}[E, QFL])dE$, will show an asymmetry in the expressions for n and p not present in the standard relations (5.2.11) and (5.2.12). This occurs because the probability function in the integral will be Fermi-Dirac form for electrons (majority carriers) and Boltzmann form for holes, and because the QDS may contain the effects of impurity banding for the electrons but not for the holes. In principle, knowledge of the QDS for both bands will permit replacing the standard relation by

$$n = A f[(E_C/-e) - v_N] \quad (5.3.1.1)$$

$$p = B f^*[v_P - (E_V/-e)] \quad (5.3.1.2)$$

These are the most general relations. If we assume that the bandtail states of the minority band are localized, f^* becomes an exponential function and B becomes the standard density of states for the valence band. If, for highly doped semiconductors, we assume impurity-banding effects are negligible, f becomes the Fermi integral of order one-half and A becomes the standard density of states for the conduction band (we allow for a deviation of the effective mass from its standard value). Otherwise f , f^* , A , and B become determined by the integral indicated above, and are known only if QDS is known.

To these two equations, we add seven more to yield ten equations in ten unknowns, suitable for finite-difference, contact-to-contact computer solution:

$$\partial n / \partial t = -\text{div}(j_N / -e) - R(n, p) + g(\text{external}) \quad (5.3.1.3)$$

$$\partial p / \partial t = -\text{div}(j_P / e) - R(n, p) + g(\text{external}) \quad (5.3.1.4)$$

$$j_N = -e \mu_n n \text{ grad}(v_N) \quad (5.3.1.5)$$

$$j_P = -e \mu_p p \text{ grad}(v_P) \quad (5.3.1.6)$$

$$\nabla^2 v = -(e/\epsilon)[p - n + N_{DD} - N_{AA} \pm \Sigma \text{trapped particles}] \quad (5.3.1.7)$$

$$E_C - E_V = E_G, \quad \text{grad}(E_C) - \text{grad}(E_V) = \text{grad}(E_G) \quad (5.3.1.8)$$

$$\text{grad}(E_C / -e) = \text{grad} v + \text{grad}(\chi / -e) \quad (5.3.1.9)$$

$$j = j_N + j_P + \partial D / \partial t, \quad D = \epsilon E, \quad E = -\text{grad}(v) \quad (5.3.1.10)$$

These equations are basic for exact computer simulation. Apparently they have not appeared as the identified basic set before, though Marshak and van Vliet (1984) discuss many relevant issues.

The equations require knowledge of many parameters such as energy-gap narrowing, minority-carrier mobility, and charged bound states. The last of these will be most important near the metallurgical junction for low forward voltage. They require also knowledge of the position dependence of the electron affinity $\chi(x)$, which apparently has received little attention, and of the quantum density of states of the majority-carrier band for moderately high concentrations (roughly $\sim 10^{18}/\text{cm}^3$) which has received most attention for the metal-insulator transition at approximately 4K.

Approximations simplify the basic equations for the quasi-neutral emitter. Just below (5.3.2) we noted that the gradient of the majority-carrier mobility edge is known, partly because of the position independence of the majority-carrier quasi-Fermi level. In the quasi-neutral emitter, low injection implies that the dependence of electric potential $v(x)$ will remain to a good approximation as it was in equilibrium. Thus Poisson's equation and the resulting entry of $\chi(x)$ can be ignored for the quasineutral emitter. This simplified computer solution. This adds emphasis, however, to a need for precise determination of the edge of the quasineutral emitter.

6. AREAL INHOMOGENEITY AND MULTIDIMENSIONAL FLOW

Apparently all detailed analyses of the highly doped emitter of silicon solar cells are based on a one-dimensional model. But the emitter surface in the best solar cells will be a mixture of ohmic-contact metal ($S \sim 10^7$ cm/s) and of a surface passivated over perhaps 95% of the area by thermal oxides or other methods that reduce the surface recombination velocity S there to orders of magnitude below 10^7 cm/s.

At least two cases of relevance exist. If the emitter is doped in the moderately high doped range ($\sim 10^{18}/\text{cm}^3$) to avoid the so-called degrading heavy-doping effects, then the relatively long diffusion lengths in this region will lead to three-dimensional minority-carrier flow. The ohmic contact metal will so reduce the minority carrier density that large minority-carrier concentration gradients will exist. Even if the design includes an n /metal contact system, partly with the motive of providing an n/n^+ low/high junction to ward minority carriers away from the ohmic contact while permitting the majority carriers to pass by the usual dielectric relaxation mechanism, this will likely not work. Because of energy gap narrowing on the n^+ side, no significant barrier in the energy band can exist at the n/n^+ junction when the doping concentration of the n side is of the order of $10^{18}/\text{cm}^3$. Thus three dimensional flow enters, and the open-circuit voltage decreases as a consequence.

In the other case, the design includes n^+ silicon over the great majority of the emitter volume. Then the diffusion length of minority carriers in the emitter will be short enough to admit estimates by neglecting three- or two-dimensional flow. In the resulting model, one-dimensional flow prevails. But over the 5% of the area covered by the ohmic contact the diode there will have a high reverse saturation current, resulting from vanishing of minority carriers at the surface. Over the remaining 95% of the area, the reverse saturation current will be much smaller because of the low S over that area. Thus, in good designs in which the recombination current of the quasineutral base is small enough that the emitter enters significantly into determining the open-circuit voltage and the efficiency, the importance of a relatively bad diode over 5% of the area becomes potentially important.

Lindholm, Mazer, Davis and Arreola (1980) have considered this issue quantitatively. The result, for their type 1 areal inhomogeneity pertinent to this discussion, is that 5% of ohmic contact metal gives performances that nearly approaches that of a solar cell for which no thermal oxide is present to passivate the front surface. This is not seen experimentally. Perhaps the reasons for this lies in the quasi-fields and in the low D and μ treated in earlier sections. Thus the work of Lindholm, et al. (1980) needs updating to help toward informed design. This updating will help decide whether decreasing ohmic contact area can lead to high efficiencies in already highly efficient silicon solar cells.

Note that the issue here is not metal shading of the incident light. Rather it is the fraction of the surface area that is covered by ohmic contact.

7. CONCLUSIONS AND RECOMMENDATIONS

The main findings discussed here are:

(a) The quantum density of states for moderately doped silicon (approximately in the range 5×10^{17} to $10^{19}/\text{cm}^3$, deviates sharply from the standard quadratic dependence on kinetic energy. This can lead to pinning of the majority-carrier quasi-Fermi level and produce thereby, for a position-dependent impurity concentration, a quasi field on the minority carriers that drifts them toward the surface. The modeling of many pertinent variables in this moderate concentration range is incomplete, although other workers, particularly Slotboom and deGraaf (1975), have emphasized this doping range. The incompleteness results from the model they and others have used, which combined Boltzmann statistics with an implicit quadratic relation between the quantum density of band states and the free-carrier kinetic energy. The metal-insulator transition dramatically illustrates the inadequacy of this quantum density of states for moderate doping concentrations. As a potential benefit, note that the long and continuing interest in the metal-insulator transition, both experimental and theoretical, provides clues for the modeling of this range of moderate doping concentrations.

(b) For higher doping concentration, experimental evidence suggests the adequacy of describing the majority carriers by a Fermi gas, that is, by a Fermi integral of order one-half. This admits use of a majority-carrier screening model, which, though much less ambitious than the many-particle computations that have and are emerging, gives simple theoretical dependencies of energy-gap narrowing on impurity concentration and temperature. These dependencies agree favorably with the experimental results on energy-gap narrowing of several different groups of workers. Compared with the many-particle model, the carrier-screening model has the virtues of simplicity and of yielding an analytic expression. This carrier-screening model in its earliest form ((Sah, Chan, Wang, Sah, Yamakawa, and Lutwak) 1981) and in its more detailed form (Landsberg, Neugroschel, Lindholm, and Sah, 1984) differs substantively from earlier carrier-screening models (Hauser, 1969), (Lanyon and Tuft, 1979).

(c) The randomness of the atomic potential contributed by the assumed random positioning of the impurity atoms leads to the formation of tails on both the conduction and valence bands. The characteristic time associated with trapping at localized states in the tail adjoining the minority-carrier band may involve a mechanism that contributes to low minority-carrier diffusivity and mobility of the Boltzmann gas describing the minority carriers. Experimental evidence exists to support this conclusion (Neugroschel and Lindholm, 1983), although contrary suggestions appear in the literature. Computer simulation of solar-cell performance requires detailed knowledge of minority-carrier diffusivity and mobility just as much as it requires such knowledge of the energy-gap narrowing. Moreover, experimental interpretation involving electrical response also requires such knowledge.

(d) The optical absorption coefficient $\alpha(\lambda)$ in moderately and highly doped silicon is highly uncertain; apparently it is also uncertain for silicon having dilute doping concentrations. Because the absorption coefficient provides suggestions about the energy-momentum relation of heavily doped silicon, it has fundamental importance to the unravelling of the detailed transport and optical properties of the material. This use we view as more significant than is the moderate need for knowing $\alpha(\lambda)$ for detailed computer simulation of solar-cell performance parameters.

(e) The results of simple models for a heavily doped region containing ohmic contacts mixed with thermal oxide suggests that the one-dimensional model conventionally used may not accurately predict the performance parameters of the emitter region, particularly the open-circuit voltage. Other sources of areal inhomogeneity also exist, such as impurity clustering (.... 1984).

(f) The basic equations for computer simulation of solar cells containing heavily doped silicon require inclusion of all of the effects described above. Present computer programs are based on equations that fall short of the status aimed for by this recommendation. Continual updating is needed as experiment and theory reveal more about the dependence of transport and quantum parameters on doping concentration, chemical species, temperature, etc. The

most severe need exists at the moderately high doping concentrations defined above. There the conventional treatment as a Fermi or Boltzmann gas fails.

(g) In their greatest generality, the basic equations for the simulation of solar-performance must include time variations. This need arises particularly because time variations of response exist in many measurements used to determine parameters. For greatest generality, one may add the Maxwell's equations to the customary continuity and current equations. Maxwell's equations admit the view of light as a wave phenomenon; when combined with the phenomenological material parameters normally introduced, reflection and transmission results. (Absorption and the optical generation rate in the continuity equations involve, at least fundamentally, the particle model of light as incident photons that produce quantum transitions between the bands or to bound states in the forbidden bands.)

(h) The basic equations include a kinetic equation of the time-rate change of occupancy at a bound state resulting from transitions from band states. This kinetic equation, emphasized by Sah (1971), is absent in most formulations of the basic equations for computer simulation. It enters markedly into such issues as the detailed modeling of minority-carrier mobility and diffusivity, discussed above. For the steady state inclusion of trap occupancy in the Poisson equation is highly important near the metallurgical p/n junction, where the donor and acceptor dopant concentrations nearly cancel (Lindholm and Sah, 1977). It is important also for work aiming toward high conversion efficiency using relatively thin and inexpensive silicon, such as that deriving from the WEB process. Most computer programs neglect the trapping mechanism, even in the steady state. The notable exception appears to be the computer simulations of Sah and co-workers (1981).

(i) The recent work of Neugroschel and Lindholm (1983) on low mobility and diffusivity of minority carriers in Si:As of doping concentration about $10^{20}/\text{cm}^3$ suggests a novel method of protection from surface recombination at both the front and back surfaces. These arise from the possibility of significant gradients in minority-carrier D and μ provoked by very highly doped silicon ($\sim 10^{21}/\text{cm}^3$ or above) in thin layers (~ 500 Å or less) near the surfaces. The work now evolving in non-equilibrium growth following eximer laser radiation (and melting) may provide a method of sealing the surfaces against minority-carrier loss. This sealing might occur despite the large impact Auger recombination rates in such n^{++} or p^{++} silicon. Experiment will decide this. The issue is the inhibiting of flow by the gradients of D and μ versus the opposing effects of energy-gap narrowing and Auger recombination. As one aspect of the issue, we may expect that the Auger recombination, if band-band, will have a rate that is proportional to n^2 (for n-type material) whereas the gradients in minority-carrier D and μ may have sufficient strength to offset this n^2 dependence by warding minority carriers away from the volume of the n^{++} region. We note that nothing is known of the physical electronics of n^{++} or p^{++} silicon, as defined above. Essentially no detailed experimental data are available about the physical electronics, and the model for energy-gap narrowing of Sec. 3.5 does not apply for concentrations greater than about $5 \times 10^{20}/\text{cm}^3$, according to Landsberg, et al. (1984).

(j) From the discussion in Sec. 5.3.1, it follows that apparently the formulation of the basic equations for finite-difference computer solutions from contact to contact remains far from complete. By this we mean to suggest that apparently computer programs now developed cannot accommodate important aspects of heavily doped silicon that physical theory and experimental studies have identified and in the future may yield values of relevant parameters.

8. REFERENCES

Blakemore, J. S., 1982, *Solid-State Electronics*, 25, 1067.

del Alamo, J. A., and R. M. Swanson, 1984, *IEEE Trans. Electron Devices*, 31, 123; Reply by A. Neugroschel and F. A. Lindholm, *ibid*, p. 124.

del Alamo, J. and R. M. Swanson, 1984, *Proc. 18th Photovoltaic Conf.*, Orlando, FL.

Fritzsche, H., 1979, *The Metal-Nonmetal Transitions in Disordered Systems*, *Proc. 19th Scottish Summer School in Physics*.

Fossum, J. G., F. A. Lindholm, and M. A. Shibib, 1979, *IEEE Trans. Electron Devices*, 26, 165.

Hauser, J. R., 1969, *NSF Final Report*.

Iles, P. and I. Sockloff, 1976, *NASA Final Report*.

Keyes, R. W., 1979, *Solid-State Communications*, 32, 179.

Keyes, R. W., 1981, *Comments Solid State Phys.*, 10, 23.

Kleppinger, D. D., 1970, *An extension of the engineering theory of semiconductors, with applications*, Ph.D. dissertation, University of Florida, Ch. 2.

Kubo, R., 1971, *Statistical Mechanics: An Advanced Course with Problems and Solutions* (North-Holland, Amsterdam, London).

Landsberg, P. T., 1952, *Proc. R. Soc. London, Ser. A*, 213, 226.

Landsberg, P. T., 1981, *Europ. J. Phys.*, 2, 213.

Landsberg, P. T., A. Neugroschel, F. A. Lindholm, and C. T. Sah, 1984, *Proc. 18th Photovoltaic Specialists Conf.*, Orlando, FL, IEEE, New York.

Lanyon, H. P. D. and R. A. Tuft, 1979, *IEEE Trans. Electron Devices*, 26, 1014.

- Lifshitz, I. M., 1941, J. Exp. Theor. Phys., 2, 117, 137, 156.
- Lindholm, F. A. and R. W. Ayers, 1968, Proc. IEEE, 56, 371.
- Lindholm, F. A., S. S. Li, and C. T. Sah, 1975, Proc. 11th Photovoltaic Specialists' Conf., Phoenix, AZ, 32, IEEE, New York.
- Lindholm, F. A. and C. T. Sah, 1977, IEEE Trans. Electron Devices.
- Lindholm, F. A., J. A. Mazer, J. R. Davis, and J. I. Arreolla, 1980, Solid-State Electron., 23, 967.
- Lindholm, F. A., 1984, Solar Cells, 12, 131.
- Marshak, A. H., and C. M. van Vliet, 1984, Proc. IEEE, 72, 148.
- Mott, N. F., 1949, Proc. Phys. Soc. (London), 62, 416.
- Mott, N. F. and W. D. Twose, 1961, Adv. Phys., 10, 107.
- Mott, N. F. and E. A. Davis, 1971, Electronic Processes in Non-Crystalline Solids (Clarendon, Oxford).
- Neugroschel, A. and F. A. Lindholm, 1983, Appl. Phys. Lett., 42, 176.
- Prigogine, I., 1980, From Being to Becoming: Time and Complexity in the Physical Sciences (Freeman, San Francisco).
- Sah, C. T., 1971, Physica Status Solidi (a), 7, 541.
- Sah, C. T. and F. A. Lindholm, 1973, Solid-State Electron., 16, 1447.
- Sah, C. T., 1977, IEEE Trans. Electron Devices, 24, 410.
- Sah, C. T., 1977, IEEE Trans. Electron Devices, 24, 358.
- Sah, C. T., P. C. Chan, A. C. Wang, R. L. Y. Sah, K. A. Yamakawa and R. Lutwak, 1981, IEEE Trans. Electron Devices, 28, 304; also see references therein.
- Shibib, M. A., F. A. Lindholm, and F. Therez, 1979, IEEE Trans. Electron Devices, 26, 959.
- Shibib, M. A. and F. A. Lindholm, 1980, IEEE Trans. Electron Devices, 27, 1304.
- Slotboom, J. and H. de Graaf, 1975, Int. Electron Devices Meeting; also Solid-State Electron., 29, 857.

9. FIGURE CAPTIONS

Fig. 1 Overlapping impurity states give rise to

Fig. 2 impurity band in the energy gap.

Fig. 3 The resistivity ρ in Ω cm at 4.2K of Si:P plotted as a function of donor concentration (Alexander and Holcomb, 1968).

Fig. 4 Density of states for an electron in an n-type semiconductor showing the splitting of the impurity band into the ϵ_3 band (a), and the ϵ_2 band (b). (c) is the conduction band.

Fig. 5 Illustrating that $\text{grad}(E_V) \neq \text{grad}(E_C)$ in the n^+ emitter. The conduction- and valence-band edges, $E_C(x)$ and $E_V(x)$, are mobility edges, the boundaries between localized and delocalized states; $E_G(x)$ is the mobility gap where disorder exists.

Fig. 6 The Einstein diffusivity-to-mobility ratio for majority carriers, under the assumption of a square root dependence of the quantum density of states on the majority carrier kinetic energy.

Fig. 7 The equilibrium product of the hole concentration P and the electron concentration N normalized by the standard square of the intrinsic concentration as a function of the reduced Fermi level, under the constraints of no energy gap narrowing and a square root dependence of the quantum density of states on the majority carrier kinetic energy. The increasing values on the abscissa correspond to increasing dopant concentration.

Fig. 8 Not present in manuscript (because of oversight).

Fig. 9 Schematic diagram showing the decomposition of the band-gap energy into W and the work done against attraction. More carriers are assumed present for curve 1 than for curve 2.

Fig. 10 Gap shrinkage ΔE_G as inferred from transport measurements for n-type layers from various sources at a mean temperature of ~ 340 K. The upper curve is for $m^*/m = 1.45$, the lower curve is for $m^*/m = 1.10$, and $\epsilon = 11.7$ (Si) has also been used. The horizontal axis is the majority carrier concentration.

Fig. 11 Comparison with recent optical data at 5 K.

Fig. 12 Qualitative illustration of the band edges of heavily doped n^+ -silicon. The broken lines show the unperturbed parabolic bands. The positions of both the electron and hole quasi-Fermi levels is also indicated. The arrows near E_V indicate hole capture and emission by

the tail states and by the acceptor level from the p-type substrates. The penetration of the tail states into the forbidden gap is assumed to be very small in comparison with the bandgap $E_G = E_C - E_V$.

Fig. 13 The band edges for the n^+ silicon in which the donor dopant concentration decreases sharply with x ($x = 0$ is the surface): - - -, band edges corresponding to the rigid band model (these illustrate a deep penetration of the Fermi level and a modest force field (nearly zero) acting on the holes); ———, band edges corresponding to a majority carrier quantum density of states warped relative to that of the rigid band model (these illustrate Fermi level saturation and a consequent strong force field drifting holes toward the surface).

ORIGINAL PAGE IS
OF POOR QUALITY

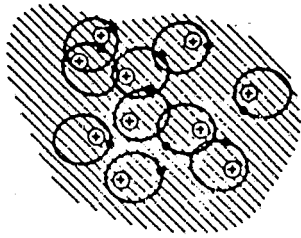


Fig. 1

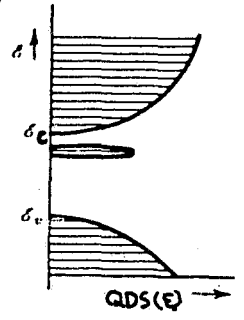


Fig. 2

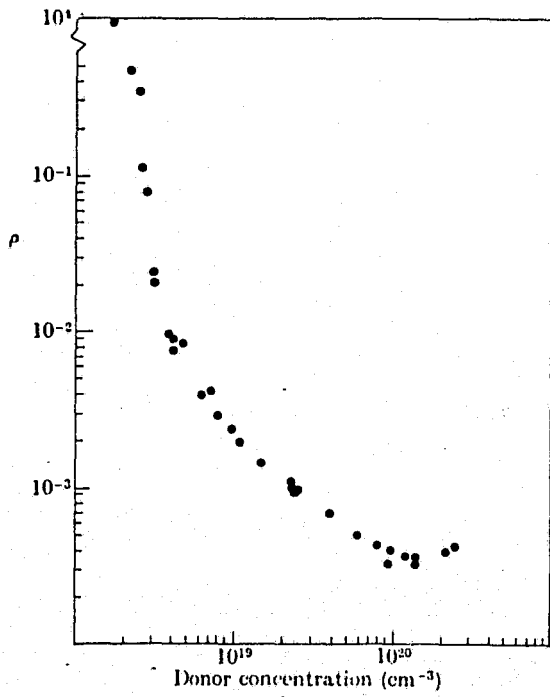


Fig. 3

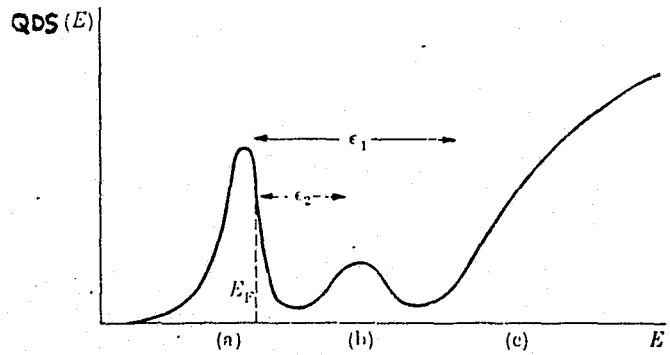


Fig. 4

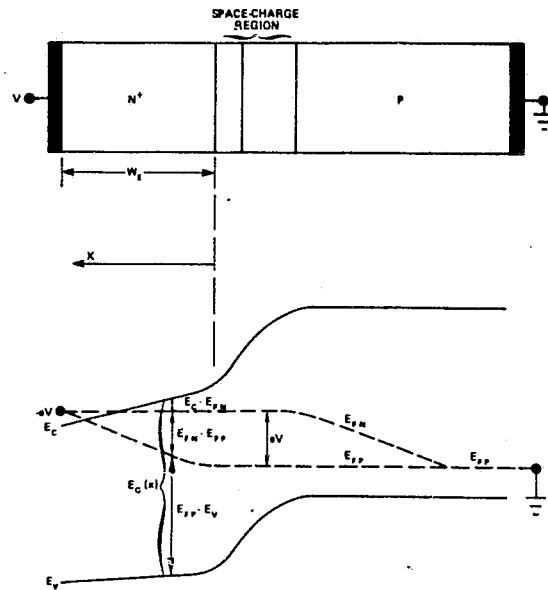


Fig. 5

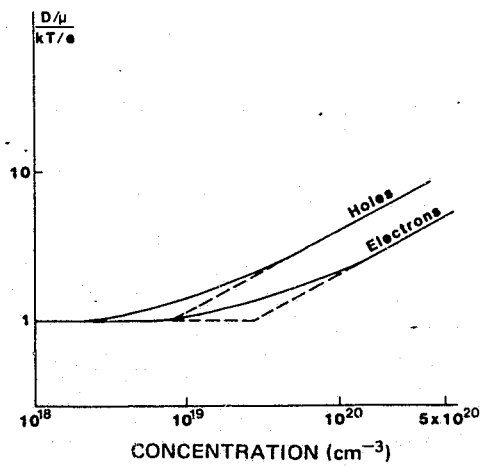


Fig. 6

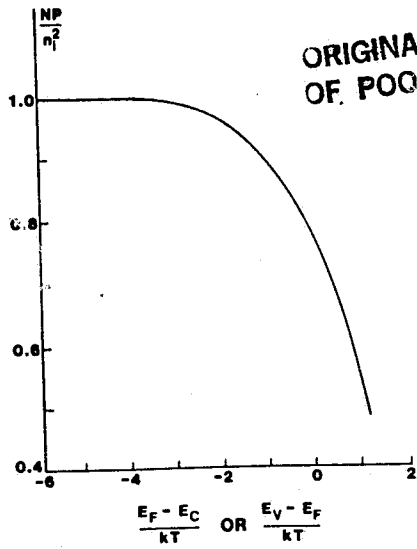


Fig. 7

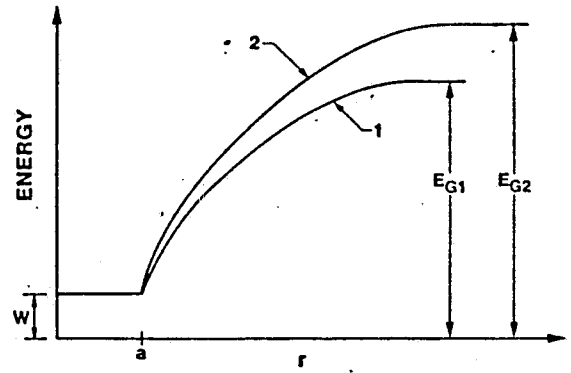


Fig. 9

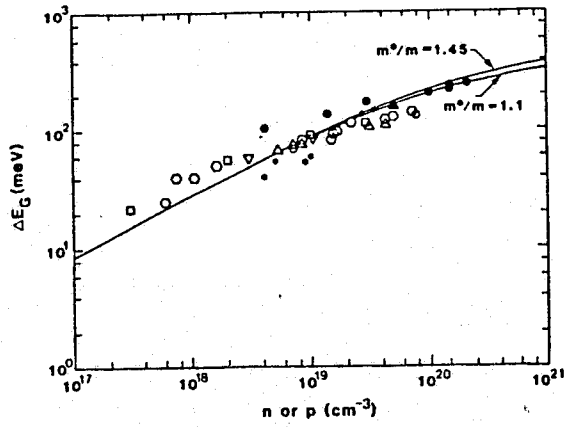


Fig. 10

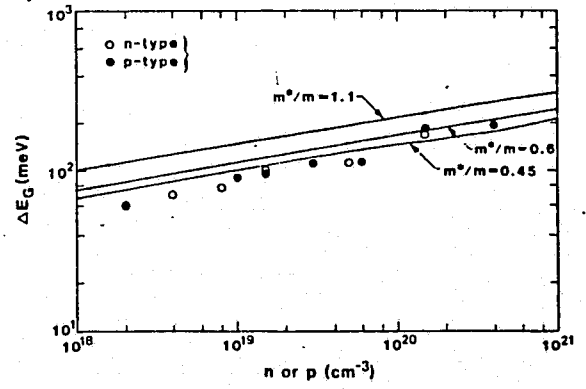


Fig. 11

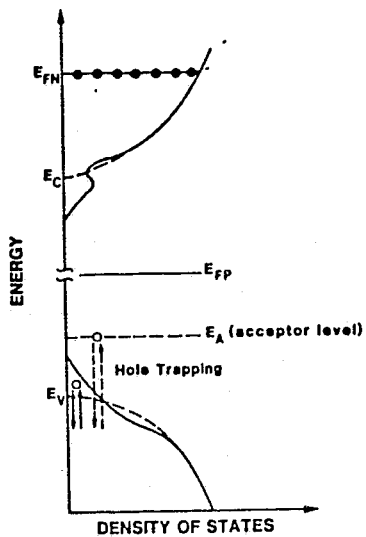


Fig. 12

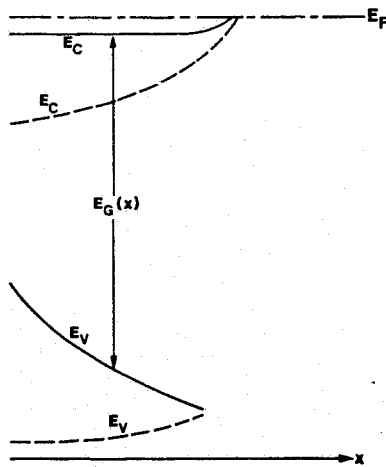


Fig. 13

DISCUSSION

QUESTION: Fred, I just have a couple of simple questions. You talk about the definition of the ohmic contact. Have we seen any such ohmic contacts?

LINDHOLM: Yes, I think in Martin Green's cell contact, the tunneling junction has a heterojunction such that there is a blocking barrier for the holes in the end-type material, yet the electrons tunnel freely into the conduction band of the metal. That would be one example. Another place -- I might just mention a very good book on contacts, which is called Photoconductivity and Allied Problems, by Albert Rose, is very good, because it is so thin. I think we should think a lot about contacts.

QUESTION: Some 30 years ago, when the effort was solving the junction equations, I worked with a mathematical physicist named Paul Wise. His opinion, unshakably, was that the quasi-Fermi level was a mathematical artifact. In other words, if your carrier concentrations were constant then you could say, yes, quasi-Fermi level was constant; if they weren't, they weren't. Rather than give a physical significance and work from there, he insisted that you just can't use it. I haven't followed the literature since then. I'm wondering if he is wrong?

LINDHOLM: Yes, he is completely wrong. The electrochemical potentials are basic thermodynamic variables. This question was asked of Peter Landsberg in a heavy-doping workshop some time ago, and I remember his answer. The electric potential we all know about; if you look in any book on the theory of heat or thermodynamics you'll find the chemical potential. And it's the algebraic sum of the two. So there's no problem, except with your friend. Oldwig (von Roos) said only in local thermal equilibrium, and it is true that the linearity between the current and the gradient and the quasi-Fermi level will not work if you have extraordinary variations in the quasi-Fermi level, but that's not surprising, because linearity -- as we know -- only applies for small perturbations, anyway. On the other hand, small perturbations can be very large currents of the sort we get with 1,000 suns with no problem at all.

SCHMIDT: You still believe in the rigid band approximation?

LINDHOLM: No, I don't. Only for doping concentrations above, say, 5×10^{19} to 10^{20} it is pretty good. Except the band edges on the minority carrier bands would be important there, even for the high doping concentrations.

SCHMIDT: You mentioned a variable electron affinity and if it affects the forces acting on carriers. Now the electron affinity is very little known, so that's a problem. However, I found some time ago that if you have low-level injection conditions and you have a variable chemical composition or doping or other facts, then the force on minority carrier is strictly the gradient of the band gap. Plus, of course, the potential force.

LINDHOLM: That is absolutely correct.

SCHMIDT: So there is no influence of the electron affinity?

LINDHOLM: This is absolutely true in low injection, and other workers have found that also and have published it. However, the low injection implies that you have a minority carrier, and that implies that you are in a quasi-neutral region. So when you get out of a quasi-neutral region and get into what people call a depletion region -- which I don't like to call it, I like to call it junction-transition region or space-charge region -- then if the gradient in the electron affinity is present, then it will introduce an effect. I can discuss that with you with this very simple picture. You probably know that anyway.

SCHMIDT: With this background, I like the way you deduced your points and you came to some conclusions. And just to make a test of it, my question is: do you question the present ideas about the Auger recombination correlated with the concentrations of certain dopants? Because, for a practical person, this is an extremely important thing. We had not been sure up to now: the correlations that you often had seen, up to the present time, of carrier concentrations or doping concentrations and the boundary of Auger recombination seem to be, let's call it, rigid. Do you think, from your point of view now, that that can be questioned?

LINDHOLM: Yes. I'm heavily opinionated on this issue also. My opinion is that the Auger coefficients are open to question. Since there has been a single experiment done at rather high doping concentration, and some of these other things I have talked about could influence these things. I would say on a theoretical level that the primary person who has worked on the theory of those Auger combinations is Peter Landsberg. And his physics is impeccable, but it involves many, many approximations. So he can only give us an estimate. So we will have to find the results from experiment, and I think it's an open question. Mainly when people talk about Auger recombination, they think about band-to-band Auger recombination but, as you know -- you have pointed out in your talks -- there are many recombination states in a diffused junction and, therefore, the Auger process may be extremely important, and that should not be overlooked. And that is only estimated, as far as I know, from a theoretical viewpoint, and by Peter Landsberg and Robbins first. You bring attention to a very important point.

SCHMIDT: I think you may have sensed why I asked you that question. For somebody who is responsible to prepare semiconductors, it is extremely important to know what kind of doping level could be tolerated and still make good solar cells.

LINDHOLM: That's an excellent point. The band-to-band Auger process gives you an ultimate upper bound. For higher doping concentrations, certainly the band-to-band Auger recombination gives you an upper bound. That needs to be looked at carefully, and experimentally, again.

SCHMIDT: Do you think that the situation may be changing again in case you have a highly counter-doped material?

LINDHOLM: Could be.